Available online at www.sciencedirect.com
SCIENCE DIRECT®
PERGAMON
International Journal of Heat and Mass Transfer 47 (2004) 101–109
International Journal of HEAT and MASS TRANSFER
www.elsevier.com/locate/ijhmt

Solution of the radiative integral transfer equations in rectangular participating and isotropically scattering inhomogeneous medium

Zekeriya Altaç *, Mesut Tekkalmaz

Department of Mechanical Engineering, School of Engineering and Architecture, Osmangazi University, 26480 Batı Meşelik, Eskişehir, Turkey

Received 24 July 2002; received in revised form 16 December 2002

Abstract

Radiative integral transfer equations for a rectangular participating and isotropically scattering inhomogeneous medium are solved numerically for the incident energy and the net partial heat fluxes using the method of "subtraction of singularity". All the relevant single (surface integrals) and double integrals (volume integrals) are carried out analytically to reduce the computation time and numerical integration errors. The resulting system of linear equations are solved iteratively. A benchmark problem is chosen as a rectangular inhomogeneous cold participating medium which is subject to externally uniform diffuse radiation on the bottom surface. Solutions for linearly and quadratically varying scattering albedos are provided in tabular form.

Keywords: Emitting; Scattering; Radiation; Participating medium

1. Introduction

The radiative transfer in multidimensional rectangular geometries has numerous application areas such as the design of combustion chambers and furnaces. In addition, if the medium is participating, the analysis is further complicated due to scattering, absorption and emission. The radiative integral transfer equation (RITE) solutions represent the exact solutions of radiative transfer problems for any geometry. Since the angular dependence of radiative transfer equation is removed through the integration of the radiation intensity over the solid angle to obtain incident energy, the RITEs contain only the spatial variables and are dimensionally simpler than other existing approximate methods. However, the RITEs have singular transfer kernels and therefore they are difficult to solve. On the other hand, in numerical solutions the system of linear equations, especially in multidimensional geometries, leads to dense matrices which result in severe limitations on the number of grid points that can be treated without incurring prohibitive requirements for the computational memory and execution time. Yet highly accurate (at least four significant digit) and comprehensive RITE solutions are sought generally for benchmarking purposes rather than to solve practical engineering applications.

A technique to solve singular integral equations of the kind we encounter in radiative transfer—the Fredholm integral equation of the second kind—is the method of "subtraction of singularity" or "removal of singularity" which was first used and validated by Layolka and Tsai [1] to solve neutron transport problems in a rectangular geometry. The method was first employed in the radiative transfer analysis of a two-dimensional rectangular medium by Crosbie and Schrenker [2], and comprehensive tabular solutions were provided for various benchmark cases. The method was also successfully employed to radiative transfer

* Corresponding author. Tel.: +90-222-239-37-50x3365; fax: +90-222-239-36-13.
E-mail addresses: zaltac@ogu.edu.tr (Z. Altaç), tmesut@ogu.edu.tr (M. Tekkalmaz).

0017-9310/$ - see front matter
doi:10.1016/S0017-9310(03)00402-2

Nomenclature

$\mathrm{Bis}_n(x,\theta)$ special function of two arguments defined by Eq. (A.4)
$\mathrm{Cis}_n(x,\theta)$ special function of two arguments defined by Eq. (A.5)
$G(x,y)$ incident energy ($=\int\int_\Omega I(x,y,\mathbf{\Omega})\,\mathrm{d}\mathbf{\Omega}$)
$I(x,y,\mathbf{\Omega})$ radiation intensity
$\mathrm{Ki}_n(x)$ Bickley–Naylor functions of nth order
N number of grid spacing
$S(x,y)$ source function defined by Eq. (4)
X, Y coordinate variables
a, b optical dimensions of the rectangular domain (in mfp)
$f(x,y)$, $g(x,y)$, $h(x,y)$ boundary integrals defined by Eqs. (5)–(7)
r polar coordinate variable
$q_x(x,y)$ net radiative heat flux in x-direction ($=\int\int_\Omega I(x,y,\mathbf{\Omega})\Omega_x\,\mathrm{d}\mathbf{\Omega}$)
$q_y(x,y)$ net radiative heat flux in y-direction ($=\int\int_\Omega I(x,y,\mathbf{\Omega})\Omega_y\,\mathrm{d}\mathbf{\Omega}$)
$(x_i, w_{x,i})$ Simpsons' quadratures for the interval $(0,a)$ using N_x intervals
$(y_i, w_{y,i})$ Simpsons' quadratures for the interval $(0,b)$ using N_y intervals
x, y optical coordinate variables ($x=\beta X$ and $y=\beta Y$)

Greek symbols
$\mathbf{\Omega}$, Ω_x, Ω_y scattering direction and its components
α dummy integration variable
ϕ_1, ϕ_2, ϕ_3, ϕ_4 angles defined by Eq. (A.6)
β extinction coefficient ($=\kappa(x,y)+\sigma(x,y)$)
$\kappa(x,y)$ spatially varying absorption coefficient
$\sigma(x,y)$ spatially varying scattering coefficient
θ polar angle
$\omega(x,y)$ spatially varying scattering albedo ($=\sigma(x,y)/\beta$)
ξ_1, ξ_2, ξ_3, ξ_4 angles defined by Eq. (A.6)

Subscripts
i, j grid point corresponding (x_i, y_j)
x belonging the x-direction/dimension
y belonging the y-direction/dimension
w wall
1 wall indices

Superscript
$'$ dummy integration variable

equations in one-dimensional RITEs in plane-parallel and cylindrical isotropic and linearly anisotropic medium by Altaç [3–5]. In literature, several studies of one-dimensional geometries involve the solution of RITEs with the Galerkin method [6,7], and it has not been extended to multidimensional geometries. The primarily disadvantage of the Galerkin method is that one has to evaluate many spatial moments of singular integrals which are difficult to carry out analytically. Recently the partition-extrapolation technique has found applications in the numerical solution of one- and two-dimensional radiative integral transfer [8,9]. However, the method also suffers from expensive memory and execution time requirement.

In the present work, the RITEs for a two-dimensional inhomogeneous participating medium with isotropic scattering are solved to establish five significant-decimal places accurate benchmark solutions. The results are provided in comprehensive tabular forms to aid future researchers and/or code developers for comparison purposes.

2. Radiative integral transfer equations in rectangular enclosures

Crosbie and Schrenker's two-dimensional radiative transfer problem of a homogeneous medium is chosen as a benchmark problem for inhomogeneous medium as well [2]; the inhomogeneous property of the medium is due to the space-dependent scattering albedo. The medium is non-emitting, absorbing and isotropically scattering. Uniform diffuse radiation is incident on the bottom surface only. All walls are cold and black. The coordinate system and the geometry are illustrated in Fig. 1.

The integral equations for the incident energy and the net partial heat fluxes in a inhomogeneous rectangular

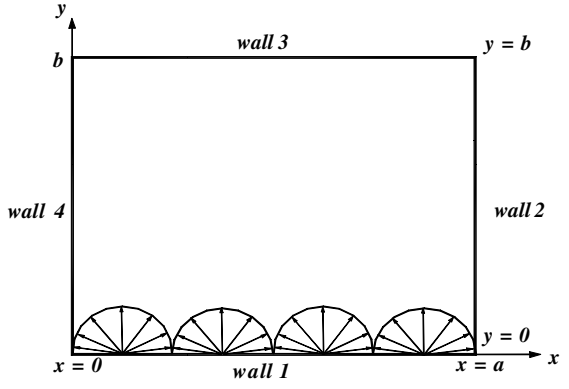

Fig. 1. Geometry and the coordinate system.

medium can be written as shown in [2] by defining $\rho = \sqrt{(x-x')^2 + (y-y')^2}$

$$G(x,y) = f(x,y) + \int_{x'=0}^{a}\int_{y'=0}^{b} S(x',y')\frac{\mathrm{Ki}_1(\rho)}{2\pi\rho}\,\mathrm{d}x'\,\mathrm{d}y' \quad (1)$$

$$q_x(x,y) = g(x,y) + \int_{x'=0}^{a}\int_{y'=0}^{b} S(x',y') \times \frac{(x-x')\,\mathrm{Ki}_2(\rho)}{2\pi\rho^2}\,\mathrm{d}x'\,\mathrm{d}y' \quad (2)$$

$$q_y(x,y) = h(x,y) + \int_{x'=0}^{a}\int_{y'=0}^{b} S(x',y') \times \frac{(y-y')\,\mathrm{Ki}_2(\rho)}{2\pi\rho^2}\,\mathrm{d}x'\,\mathrm{d}y' \quad (3)$$

with

$$S(x,y) = \omega(x,y)G(x,y) \quad (4)$$

where x and y are the optical dimensions and are defined as $x = \beta X$ and $y = \beta Y$, $\mathrm{Ki}_n(\rho)$ is the nth order Bickley–Naylor functions [10], $\omega(x,y)$ is the space-dependent scattering albedo which is given by $\sigma(x,y)/\beta$ where $\beta = \sigma(x,y) + \kappa(x,y)$ is the extinction coefficient while $\sigma(x,y)$ and $\kappa(x,y)$ are the space-dependent scattering and absorption coefficients, respectively, $S(x,y)$ is the isotropic source function, for non-emitting medium, which is defined as while $f(x,y)$, $g(x,y)$ and $h(x,y)$ are functions representing contributions of energy and flux from diffuse walls. Defining $\rho_w = \sqrt{(x-x')^2 + y^2}$, we can write these contributions for wall 1 as

$$f(x,y) = \int_{x'=0}^{a} I_{w_1}(x')\frac{y\,\mathrm{Ki}_2(\rho_w)}{2\pi\rho_w^2}\,\mathrm{d}x' \quad (5)$$

$$g(x,y) = \int_{x'=0}^{a} I_{w_1}(x')\frac{y(x-x')\,\mathrm{Ki}_3(\rho_w)}{2\pi\rho_w^3}\,\mathrm{d}x' \quad (6)$$

$$h(x,y) = \int_{x'=0}^{a} I_{w_1}(x')\frac{y^2\,\mathrm{Ki}_3(\rho_w)}{2\pi\rho_w^3}\,\mathrm{d}x' \quad (7)$$

where $I_{w_1}(x)$ is the diffuse radiation intensity of the bottom wall (wall 1).

To solve the integral equations using the "subtraction of singularity", Eqs. (1)–(3), we subtract the singularity at $(x,y) = (x',y')$ as follows

$$G(x,y) = f(x,y) + \int_{x'=0}^{a}\int_{y'=0}^{b}\left[S(x',y') - S(x,y)\right] \times \frac{\mathrm{Ki}_1(\rho)}{2\pi\rho}\,\mathrm{d}x'\,\mathrm{d}y' + \frac{1}{2\pi}S(x,y)H(x,y) \quad (8)$$

$$q_x(x,y) = g(x,y) + \int_{x'=0}^{a}\int_{y'=0}^{b}\left[S(x',y') - S(x,y)\right] \times \frac{(x-x')\,\mathrm{Ki}_2(\rho)}{2\pi\rho^2}\,\mathrm{d}x'\,\mathrm{d}y' + \frac{1}{2\pi}S(x,y)U(x,y) \quad (9)$$

$$q_y(x,y) = h(x,y) + \int_{x'=0}^{a}\int_{y'=0}^{b}\left[S(x',y') - S(x,y)\right] \times \frac{(y-y')\,\mathrm{Ki}_2(\rho)}{2\pi\rho^2}\,\mathrm{d}x'\,\mathrm{d}y' + \frac{1}{2\pi}S(x,y)V(x,y) \quad (10)$$

where

$$H(x,y) = \int_{x'=0}^{a}\int_{y'=0}^{b}\frac{\mathrm{Ki}_1(\rho)}{\rho}\,\mathrm{d}x'\,\mathrm{d}y' \quad (11)$$

$$U(x,y) = \int_{x'=0}^{a}\int_{y'=0}^{b}(x-x')\frac{\mathrm{Ki}_2(\rho)}{\rho^2}\,\mathrm{d}x'\,\mathrm{d}y' \quad (12)$$

$$V(x,y) = \int_{x'=0}^{a}\int_{y'=0}^{b}(y-y')\frac{\mathrm{Ki}_2(\rho)}{\rho^2}\,\mathrm{d}x'\,\mathrm{d}y' \quad (13)$$

In Eqs. (8)–(10), in case of $(x',y') \to (x,y)$, the terms under the double integral signs will vanish. Thus, the singularities are effectively dealt with. The exact evaluation of the boundary integrals, Eqs. (5)–(7), and the double integrals, Eqs. (11)–(13), are given in detail in Appendix A.

3. Numerical solution method

We divide $x \in (0,a)$ and $y \in (0,b)$ to N_x and N_y equal grid segments, respectively, and generate Simpson's integration quadratures which are taken to be $(x_i, w_{x,i})$ for $i = 1,\ldots,N_x$ and $(y_i, w_{y,i})$ for $i = 1,\ldots,N_y$ where $(x_i, w_{x,i})$ and $(y_i, w_{y,i})$ are corresponding abscissas and weights. Then the double integrals are replaced by the quadrature summations and using a short hand notation, for example $G(x_i,y_j) = G_{i,j}$, for the known and/or unknown quantities; we can write Eqs. (8)–(10) as

$$G_{i,j} = f_{i,j} + \sum_{\substack{m,n=1\\ m,n\neq i,j}}^{N_x,N_y} w_{x,m}w_{y,n}\left[\omega_{m,n}G_{m,n} - \omega_{i,j}G_{i,j}\right] \times \frac{\mathrm{Ki}_1(\rho_{m,n,i,j})}{2\pi\rho_{m,n,i,j}} + \frac{1}{2\pi}\omega_{i,j}G_{i,j}H_{i,j} \quad (14)$$

$$q_{x_{i,j}} = g_{i,j} + \sum_{\substack{m,n=1\\ m,n\neq i,j}}^{N_x,N_y} w_{x,m}w_{y,n}\left[\omega_{m,n}G_{m,n} - \omega_{i,j}G_{i,j}\right] \times \frac{(x_i - x_m)\,\mathrm{Ki}_2(\rho_{m,n,i,j})}{2\pi\rho_{m,n,i,j}^2} + \frac{1}{2\pi}\omega_{i,j}G_{i,j}U_{i,j} \quad (15)$$

$$q_{y_{i,j}} = h_{i,j} + \sum_{\substack{m,n=1\\ m,n\neq i,j}}^{N_x,N_y} w_{x,m}w_{y,n}\left[\omega_{m,n}G_{m,n} - \omega_{i,j}G_{i,j}\right] \times \frac{(y_j - y_n)\,\mathrm{Ki}_2(\rho_{m,n,i,j})}{2\pi\rho_{m,n,i,j}^2} + \frac{1}{2\pi}\omega_{i,j}G_{i,j}V_{i,j} \quad (16)$$

where $\rho_{m,n,i,j} = \sqrt{(x_i - x_m)^2 + (y_j - y_n)^2}$.

Now Eq. (14) can be rearranged to constitute a system of linear equations which need to be solved for the incident energy within the domain. Direct solution of this dense system through Gauss-elimination is possible if relatively small number of intervals are used (10–30). In this case, the dense matrices which is also computationally involved is established only once. For large number of intervals, not only computation time but also memory restrictions are to be overcome. In this case, to obtain highly accurate solutions through using large number of grids ($N > 30$), we have used an iterative algorithm to avoid memory restrictions due mainly from the storage of the resulting matrices. A double precision computer program was written and compiled with Lahey Fortran Compiler. The convergence was determined when the maximum error of the two consecutive iterations of the incident energy was less than 10^{-6}; the net partial heat fluxes were computed using Eqs. (15) and (16) after converged solutions for the incident energy was obtained.

4. Results and discussion

In this study, the exact integral equation solutions for space-dependent scattering albedos of $\omega(x,y) = 0.5(x/a + y/b)$, $\omega(x,y) = 1 - 0.5(x/a + y/b)$, $\omega(x,y) = 0.7 - 0.3(x^2/a^2 + y^2/b^2)$ and $\omega(x,y) = 0.3(1 + x^2/a^2 + y^2/b^2)$ are sought for square enclosures of 0.5×0.5, 1×1 and 2.5×2.5 in mean-free-path (mfp) dimensions. In addition, solutions for rectangular enclosures of 0.5×1, 0.5×2, 0.5×4, 1×0.5, 2×0.5, and 4×0.5 in mfp and the spatially varying scattering albedo of $\omega(x,y) = 0.7 - 0.3(x^2/a^2 + y^2/b^2)$ are obtained and tabulated. The average value $\omega(x,y)$ over the rectangular medium is equal to 0.5 in all cases.

The RITE solutions for homogeneous medium given by Crosbie and Schrenker [2] were used to validate the computer code for various geometry and constant scattering albedo configurations. Our solutions were in excellent agreement (five significant digit accuracy) with those provided by Crosbie and Schrenker [2]. The DOM solutions for all cases were also obtained to cross-check and validate the exact RITE solutions in inhomogeneous medium. In the DOM, the diamond-difference scheme [11] and level symmetric S_{16} quadratures [12] were adapted.

In Table 1, the effect of grid refinement on the exact and discrete ordinate method S_{16} solutions are given for a square medium of 2.5 mfp$\times$2.5 mfp with $\omega(x,y) = 0.7 - 0.3(x^2/a^2 + y^2/b^2)$. Since the numerical integration error of Simpsons' rule is fourth order, very accurate solutions for the optically thin medium can be expected with relatively small number of grids. As a result, in square enclosures the 100×100 and in rectangular enclosures the 40×100 or the 100×40 grid configuration was used to ensure five-decimal places accuracy in the solutions. The discrepancies of the DOM solutions are due to the ray effect (unphysical oscillations in the solutions) and false scattering which is unavoidable in multidimensional geometries.

In Table 2, the RITE solutions for the incident energy and the partial heat fluxes are tabulated for selected points on the bottom, top and east walls for 0.5×0.5, 1×1, and 2.5×2.5 (in mfp dimensions) square enclosures having a space-dependent scattering albedo of $\omega(x,y) = 0.5(x/a + y/b)$. In Table 3, the solutions for the same geometries are repeated for a medium having a scattering albedo of $\omega(x,y) = 1 - 0.5(x/a + y/b)$.

In Tables 4 and 5, the RITE solutions for the incident energy and the partial heat fluxes are tabulated for selected points on the bottom, top and east walls for 0.5×0.5, 1×1, and 2.5×2.5 square enclosures having space-dependent scattering albedos of $\omega(x,y) = 0.7 - 0.3(x^2/a^2 + y^2/b^2)$ and $\omega(x,y) = 0.3(1 + x^2/a^2 + y^2/b^2)$, respectively.

In Tables 6 and 7, the RITE solutions for the incident energy and the partial heat fluxes are tabulated for selected points on the bottom, top and east walls for the rectangular enclosures having a space-dependent scattering albedo of $\omega(x,y) = 0.7 - 0.3(x^2/a^2 + y^2/b^2)$.

5. Conclusion

Exact integral equation solutions using the method of subtraction of singularity for the incident energy and the net partial heat fluxes of rectangular participating and isotropically scattering inhomogeneous medium are obtained. Results are presented in tabular form in five-

Table 1
Effect of grid refinement and validation (2.5 mfp$\times$2.5 mfp, $x = 1.25$, $y = 1.25$)

	Method					
	RITE			DOM S_{16}		
	20×20	50×50	100×100	20×20	50×50	100×100
$G(x,y)$	0.11024	0.09218	0.09218	0.08866	0.09102	0.09165
$q_x(x,y)$	0.01256	0.01089	0.01091	0.01082	0.01034	0.01031
$q_y(x,y)$	0.23113	0.19926	0.19936	0.21152	0.20394	0.20326

Table 2
Exact solutions for the scattering albedo case of $\omega(x,y) = 0.5(x/a + y/b)$

x/a	Geometry								
	$a = 0.5$, $b = 0.5$			$a = 1$, $b = 1$			$a = 2.5$, $b = 2.5$		
	G	$4q_x$	$4q_y$	G	$4q_x$	$4q_y$	G	$4q_x$	$4q_y$
Bottom wall									
0.00	0.50890	−0.51985	0.98552	0.50992	−0.52367	0.98400	0.50667	−0.51735	0.98991
0.25	0.51557	−0.02005	0.97093	0.52067	−0.02655	0.96164	0.52223	−0.02444	0.96042
0.50	0.52174	−0.01113	0.95778	0.53120	−0.01672	0.94023	0.53925	−0.02012	0.92877
0.75	0.52466	0.00641	0.95187	0.53694	0.00668	0.92873	0.55170	0.00065	0.90490
1.00	0.51695	0.53213	0.96989	0.52378	0.54768	0.95817	0.52990	0.56422	0.94987
Top wall									
0.00	0.06752	−0.08947	0.19632	0.03827	−0.05409	0.11167	0.00740	−0.01142	0.02157
0.25	0.08242	−0.05626	0.24899	0.05019	−0.03642	0.15040	0.01185	−0.00917	0.03447
0.50	0.08907	−0.00507	0.27199	0.05618	−0.00590	0.16925	0.01478	−0.00316	0.04263
0.75	0.08536	0.04970	0.25680	0.05414	0.02925	0.16085	0.01480	0.00587	0.04214
1.00	0.07051	0.09174	0.20409	0.04210	0.05790	0.12155	0.00987	0.01483	0.02786
y/b									
East side wall									
0.10	0.22372	0.42733	0.43564	0.20864	0.39719	0.39552	0.16564	0.31142	0.31720
0.25	0.18234	0.32912	0.38624	0.15577	0.28123	0.31881	0.09662	0.17250	0.19563
0.50	0.13353	0.21855	0.31216	0.10184	0.16990	0.22524	0.04552	0.07734	0.09318
0.75	0.09857	0.14592	0.25095	0.06778	0.10505	0.16222	0.02286	0.03784	0.04773
0.90	0.08155	0.11298	0.22114	0.05220	0.07678	0.13557	0.01469	0.02377	0.03382

Table 3
Exact solutions for the scattering albedo case of $\omega(x,y) = 1 - 0.5(x/a + y/b)$

x/a	Geometry								
	$a = 0.5$, $b = 0.5$			$a = 1$, $b = 1$			$a = 2.5$, $b = 2.5$		
	G	$4q_x$	$4q_y$	G	$4q_x$	$4q_y$	G	$4q_x$	$4q_y$
Bottom wall									
0.00	0.52934	−0.56050	0.95502	0.54572	−0.59787	0.92871	0.56903	−0.65329	0.89030
0.25	0.54691	−0.01777	0.91871	0.57830	−0.02432	0.86292	0.63383	−0.02006	0.76397
0.50	0.54531	0.01221	0.92291	0.57426	0.02013	0.87272	0.61999	0.03087	0.79363
0.75	0.53690	0.03258	0.93969	0.55877	0.04775	0.90264	0.59019	0.05436	0.84855
1.00	0.52058	0.54704	0.97199	0.52942	0.56954	0.95914	0.53645	0.58783	0.94784
Top wall									
0.00	0.06985	−0.0883	0.20636	0.04145	−0.05420	0.12426	0.00964	−0.01312	0.02940
0.25	0.08298	−0.04854	0.25640	0.05137	−0.02818	0.16024	0.01327	−0.00561	0.04159
0.50	0.08642	0.00497	0.27144	0.05316	0.00571	0.16860	0.01326	0.00298	0.04232
0.75	0.08019	0.05506	0.24882	0.04777	0.03531	0.15032	0.01081	0.00890	0.03461
1.00	0.06694	0.08632	0.19864	0.03780	0.05109	0.11442	0.00736	0.01052	0.02302
y/b									
East side wall									
0.10	0.22639	0.44108	0.44285	0.21281	0.41721	0.40445	0.17013	0.33186	0.32524
0.25	0.18256	0.33722	0.39804	0.15611	0.29214	0.33404	0.09630	0.18042	0.20818
0.50	0.12980	0.21598	0.32379	0.09660	0.16534	0.23913	0.04043	0.07076	0.10111
0.75	0.09286	0.13688	0.25593	0.06030	0.09265	0.16711	0.01727	0.02773	0.04871
0.90	0.07621	0.10381	0.22023	0.04553	0.06495	0.13348	0.01035	0.01558	0.03117

decimal places to aid researchers and/or code developers. Pertinent surface and volume integrals for rectangular geometry which are singular in nature can be analytically evaluated through special functions. This

Table 4
Exact solutions for the scattering albedo case of $\omega(x,y) = 0.7 - 0.3(x^2/a^2 + y^2/b^2)$

x/a	Geometry								
	$a = 0.5$, $b = 0.5$			$a = 1$, $b = 1$			$a = 2.5$, $b = 2.5$		
	G	$4q_x$	$4q_y$	G	$4q_x$	$4q_y$	G	$4q_x$	$4q_y$
Bottom wall									
0.00	0.52402	−0.55005	0.96280	0.53569	−0.57741	0.94408	0.54854	−0.60948	0.92356
0.25	0.53928	−0.01942	0.93069	0.56331	−0.02702	0.88756	0.60024	−0.02576	0.82250
0.50	0.53992	0.00716	0.92976	0.56380	0.01153	0.88736	0.59785	0.01649	0.82861
0.75	0.53342	0.02810	0.94299	0.55215	0.04039	0.91027	0.57691	0.04386	0.86755
1.00	0.51890	0.54218	0.97275	0.52638	0.56122	0.96147	0.53111	0.57435	0.95412
Top wall									
0.00	0.06920	−0.08838	0.20400	0.04053	−0.05395	0.12110	0.00891	−0.01249	0.02705
0.25	0.08276	−0.05053	0.25493	0.05094	−0.03037	0.15808	0.01274	−0.00665	0.03962
0.50	0.08696	0.00299	0.27196	0.05371	0.00343	0.16905	0.01342	0.00176	0.04224
0.75	0.08108	0.05443	0.25037	0.04876	0.03459	0.15211	0.01127	0.00853	0.03548
1.00	0.06746	0.08718	0.19939	0.03835	0.05203	0.11526	0.00758	0.01092	0.02340
y/b									
East side wall									
0.10	0.22485	0.43646	0.44061	0.20998	0.40928	0.40135	0.16522	0.31934	0.32133
0.25	0.18200	0.33510	0.39438	0.15500	0.28858	0.32884	0.09443	0.17551	0.20244
0.50	0.13045	0.21695	0.32107	0.09737	0.16656	0.23567	0.04087	0.07158	0.09856
0.75	0.09382	0.13871	0.25516	0.06143	0.09488	0.16629	0.01790	0.02903	0.04836
0.90	0.07700	0.10531	0.22046	0.04641	0.06667	0.13378	0.01077	0.01643	0.03136

Table 5
Exact solutions for the scattering albedo case of $\omega(x,y) = 0.3(1 + x^2/a^2 + y^2/b^2)$

x/a	Geometry								
	$a = 0.5$, $b = 0.5$			$a = 1$, $b = 1$			$a = 2.5$, $b = 2.5$		
	G	$4q_x$	$4q_y$	G	$4q_x$	$4q_y$	G	$4q_x$	$4q_y$
Bottom wall									
0.00	0.51353	−0.52903	0.97888	0.51776	−0.53988	0.97240	0.51942	−0.54515	0.97052
0.25	0.52224	−0.01862	0.96067	0.53243	−0.02463	0.94296	0.54296	−0.02197	0.92638
0.50	0.52651	−0.00682	0.95190	0.53965	−0.01044	0.92884	0.55421	−0.01320	0.90618
0.75	0.52782	0.01026	0.94899	0.54262	0.01219	0.92237	0.56230	0.00622	0.88986
1.00	0.51847	0.53658	0.96930	0.52644	0.55492	0.95624	0.53463	0.57580	0.94416
Top wall									
0.00	0.06802	−0.08919	0.19831	0.03886	−0.05395	0.11395	0.00772	−0.01154	0.02270
0.25	0.08247	−0.05418	0.25004	0.05023	−0.03405	0.15154	0.01185	−0.00799	0.03495
0.50	0.08832	−0.00303	0.27099	0.05513	−0.00350	0.16764	0.01396	−0.00181	0.04109
0.75	0.08422	0.05024	0.25470	0.05255	0.02975	0.15771	0.01352	0.00603	0.03934
1.00	0.06981	0.09053	0.20298	0.04114	0.05617	0.11987	0.00916	0.01346	0.02643
y/b									
East side wall									
0.10	0.22509	0.43151	0.43801	0.21106	0.40396	0.39887	0.16990	0.32188	0.32141
0.25	0.18272	0.33080	0.38997	0.15642	0.28362	0.32415	0.09777	0.17535	0.20143
0.50	0.13265	0.21706	0.31490	0.10050	0.16739	0.22873	0.04414	0.07435	0.09567
0.75	0.09736	0.14352	0.25158	0.06601	0.10144	0.16270	0.02126	0.03442	0.04756
0.90	0.08052	0.11099	0.22063	0.05076	0.07390	0.13460	0.01352	0.02130	0.03273

analytical treatment reduces computation time significantly and the accuracy of the integrals can be controlled by the user. The method is suitable to produce benchmark problems of high accuracy.

Table 6
Exact solutions for the scattering albedo case of $\omega(x,y) = 0.7 - 0.3(x^2/a^2 + y^2/b^2)$

x/a	Geometry								
	$a = 0.5$, $b = 1$			$a = 0.5$, $b = 2$			$a = 0.5$, $b = 4$		
	G	$4q_x$	$4q_y$	G	$4q_x$	$4q_y$	G	$4q_x$	$4q_y$
Bottom wall									
0.00	0.52582	−0.55262	0.95823	0.52654	−0.55350	0.95647	0.52705	−0.55428	0.95551
0.25	0.54136	−0.02070	0.92505	0.54205	−0.02108	0.92321	0.54237	−0.02113	0.92271
0.50	0.54209	0.00736	0.92380	0.54280	0.00739	0.92187	0.54310	0.00740	0.92132
0.75	0.53543	0.02967	0.93759	0.53609	0.03010	0.93581	0.53638	0.03019	0.93532
1.00	0.52056	0.54472	0.96856	0.52119	0.54553	0.96699	0.52154	0.54608	0.96632
Top wall									
0.00	0.02420	−0.02107	0.07799	0.00434	−0.00241	0.01482	0.00026	−0.00009	0.00091
0.25	0.02645	−0.01074	0.08648	0.00456	−0.00113	0.01558	0.00027	−0.00004	0.00094
0.50	0.02695	0.00109	0.08870	0.00459	0.00019	0.01571	0.00027	0.00001	0.00094
0.75	0.02590	0.01229	0.08495	0.00447	0.00141	0.01533	0.00026	0.00006	0.00093
1.00	0.02359	0.02094	0.07629	0.00424	0.00241	0.01454	0.00025	0.00009	0.00090
y/b									
East side wall									
0.10	0.19716	0.36933	0.40480	0.15303	0.26601	0.34292	0.09453	0.13993	0.23751
0.25	0.13403	0.22387	0.31621	0.07465	0.10203	0.19611	0.02661	0.02682	0.07597
0.50	0.07290	0.09878	0.19765	0.02599	0.02569	0.07608	0.00476	0.00337	0.01464
0.75	0.04102	0.04541	0.12191	0.01023	0.00788	0.03212	0.00106	0.00058	0.00343
0.90	0.02942	0.02875	0.09187	0.00603	0.00398	0.01983	0.00045	0.00021	0.00151

Table 7
Exact solutions for the scattering albedo case of $\omega(x,y) = 0.7 - 0.3(x^2/a^2 + y^2/b^2)$

x/a	Geometry								
	$a = 1$, $b = 0.5$			$a = 2$, $b = 0.5$			$a = 4$, $b = 0.5$		
	G	$4q_x$	$4q_y$	G	$4q_x$	$4q_y$	G	$4q_x$	$4q_y$
Bottom wall									
0.00	0.53181	−0.57063	0.95336	0.53658	−0.58484	0.94882	0.53823	−0.59110	0.94803
0.25	0.55777	−0.02331	0.90183	0.57524	−0.01874	0.87769	0.58725	−0.00756	0.86373
0.50	0.55791	0.01063	0.90264	0.57313	0.01232	0.88343	0.58110	0.01028	0.87555
0.75	0.54708	0.03557	0.92304	0.55805	0.03283	0.90904	0.56405	0.02073	0.90250
1.00	0.52298	0.55469	0.96925	0.52356	0.55794	0.97006	0.52194	0.55440	0.97239
Top wall									
0.00	0.09260	−0.15102	0.24890	0.10276	−0.18247	0.26153	0.10526	−0.19053	0.26369
0.25	0.13368	−0.08914	0.38442	0.18090	−0.07664	0.48807	0.21101	−0.02868	0.54071
0.50	0.14583	0.00670	0.42389	0.19322	0.00970	0.51440	0.21228	0.00884	0.53801
0.75	0.12871	0.09654	0.37192	0.17031	0.08657	0.46447	0.19463	0.03921	0.50855
1.00	0.08820	0.14511	0.23847	0.09488	0.16819	0.24527	0.09448	0.16822	0.24368
y/b									
East side wall									
0.10	0.23220	0.46021	0.43822	0.23337	0.46550	0.43870	0.23168	0.46135	0.44001
0.25	0.19416	0.37480	0.39676	0.19638	0.38374	0.39713	0.19480	0.37978	0.39774
0.50	0.14860	0.27451	0.33724	0.15262	0.28952	0.33871	0.15131	0.28647	0.33814
0.75	0.11463	0.20108	0.28524	0.12019	0.22099	0.28910	0.11930	0.21937	0.28776
0.90	0.09803	0.16579	0.25665	0.10432	0.18782	0.26224	0.10372	0.18718	0.26069

Appendix A

The boundary integrals, Eqs. (5)–(7), are evaluated upon $x - x' = y\tan\alpha$ substitution. Eq. (5), yields

$$f(x,y) = \frac{1}{2\pi}\left\{\mathrm{Bis}_2\left(y, \tan^{-1}\left(\frac{x}{y}\right)\right) + \mathrm{Bis}_2\left(y, \tan^{-1}\left(\frac{a-x}{y}\right)\right)\right\} \tag{A.1}$$

Similarly, using the same substitution, we obtain

$$g(x,y) = \frac{1}{2\pi}\left\{\mathrm{Cis}_3\left(y, \tan^{-1}\left(\frac{x}{y}\right)\right) - \mathrm{Cis}_3\left(y, \tan^{-1}\left(\frac{a-x}{y}\right)\right)\right\} \tag{A.2}$$

and

$$h(x,y) = \frac{1}{2\pi}\left\{\mathrm{Bis}_3\left(y, \tan^{-1}\left(\frac{x}{y}\right)\right) + \mathrm{Bis}_3\left(y, \tan^{-1}\left(\frac{a-x}{y}\right)\right)\right\} \tag{A.3}$$

where

$$\mathrm{Bis}_n(x,\theta) = \int_{\alpha=0}^{\theta} \mathrm{Ki}_n(x\sec\alpha)(\cos\alpha)^{n-2}\,\mathrm{d}\alpha \tag{A.4}$$

and

$$\mathrm{Cis}_n(x,\theta) = \int_{\alpha=0}^{\theta} \mathrm{Ki}_n(x\sec\alpha)\sin\alpha(\cos\alpha)^{n-3}\,\mathrm{d}\alpha \tag{A.5}$$

which can be evaluated from their exact series expansions [13].

To evaluate the double integrals, Eqs. (11)–(13), we transform these into polar coordinates by taking $x' - x = r\cos\theta$ and $y' - y = r\sin\theta$. The area element becomes $\mathrm{d}x'\,\mathrm{d}y' = r\,\mathrm{d}r\,\mathrm{d}\theta$. The integration domain is depicted in Fig. 2. The r integration is simple and straightforward since $\int_0^{r_i}\mathrm{Ki}_1(r)\,\mathrm{d}r = 1 - \mathrm{Ki}_2(r_i)$, referring to Fig. 2, we can split the integrations into four triangular regions as,

$$\begin{aligned}
&r_1 = (a-x)/\cos\theta, \quad r_2 = (b-y)/\sin\theta\\
&r_3 = -x/\cos\theta, \quad r_4 = -y/\sin\theta\\
&\phi_1 = \tan^{-1}[y/(a-x)], \quad \xi_1 = \tan^{-1}[(b-y)/(a-x)]\\
&\phi_2 = \tan^{-1}[(a-x)/(b-y)], \quad \xi_2 = \tan^{-1}[x/(b-y)]\\
&\phi_3 = \tan^{-1}[(b-y)/x], \quad \xi_3 = \tan^{-1}[y/x]\\
&\phi_4 = \tan^{-1}[x/y], \quad \xi_4 = \tan^{-1}[(a-x)/y]
\end{aligned} \tag{A.6}$$

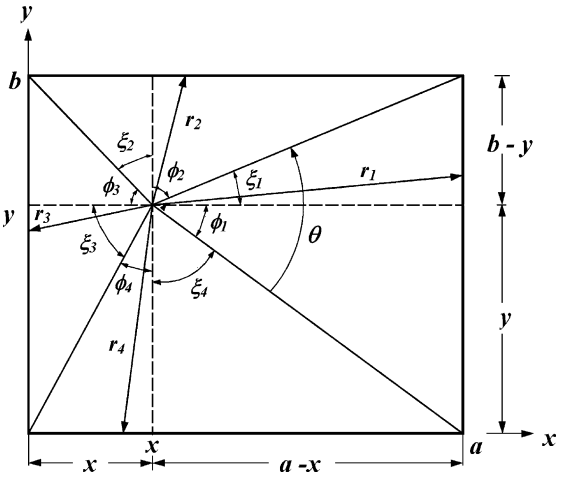

Fig. 2. Schematic for polar integration.

Finally, Eq. (11) is written as

$$\begin{aligned}
H(x,y) = &\int_{-\phi_1}^{\xi_1}\{1 - \mathrm{Ki}_2[(a-x)/\cos\theta]\}\,\mathrm{d}\theta\\
&+ \int_{\xi_1}^{\pi/2+\xi_2}\{1 - \mathrm{Ki}_2[(b-y)/\sin\theta]\}\,\mathrm{d}\theta\\
&+ \int_{\pi/2+\xi_2}^{\pi+\xi_3}\{1 - \mathrm{Ki}_2[-x/\cos\theta]\}\,\mathrm{d}\theta\\
&+ \int_{\pi+\xi_3}^{3\pi/2+\xi_4}\{1 - \mathrm{Ki}_2[-y/\sin\theta]\}\,\mathrm{d}\theta
\end{aligned} \tag{A.7}$$

Also noting that $\phi_2 + \xi_1 = \pi/2$, $\phi_3 + \xi_2 = \pi/2$ and so on, we can rewrite Eq. (A.7) as

$$\begin{aligned}
H(x,y) = 2\pi &- \int_0^{\phi_1}\mathrm{Ki}_2[(a-x)/\cos\theta]\,\mathrm{d}\theta\\
&- \int_0^{\xi_1}\mathrm{Ki}_2[(a-x)/\cos\theta]\,\mathrm{d}\theta\\
&- \int_0^{\phi_2}\mathrm{Ki}_2[(b-y)/\cos\theta]\,\mathrm{d}\theta\\
&- \int_0^{\xi_2}\mathrm{Ki}_2[(b-y)/\cos\theta]\,\mathrm{d}\theta\\
&- \int_0^{\phi_3}\mathrm{Ki}_2[x/\cos\theta]\,\mathrm{d}\theta - \int_0^{\xi_3}\mathrm{Ki}_2[x/\cos\theta]\,\mathrm{d}\theta\\
&- \int_0^{\phi_4}\mathrm{Ki}_2[y/\cos\theta]\,\mathrm{d}\theta - \int_0^{\xi_4}\mathrm{Ki}_2[y/\cos\theta]\,\mathrm{d}\theta
\end{aligned} \tag{A.8}$$

Using Eqs. (A.4) and (A.5), an exact expression for Eq. (A.8) is found to be

$$H(x,y) = 2\pi - \mathrm{Bis}_2(a-x,\phi_1) - \mathrm{Bis}_2(a-x,\xi_1) - \mathrm{Bis}_2(b-y,\phi_2) - \mathrm{Bis}_2(b-y,\xi_2) - \mathrm{Bis}_2(x,\phi_3) - \mathrm{Bis}_2(x,\xi_3) - \mathrm{Bis}_2(y,\phi_4) - \mathrm{Bis}_2(y,\xi_4) \quad (A.9)$$

Similarly, using the same integration procedure for $U(x,y)$ and $V(x,y)$, we arrive at

$$U(x,y) = -\frac{\pi}{4}\sin\phi_1 - \frac{\pi}{4}\sin\xi_1 + \mathrm{Bis}_3(a-x,\phi_1) + \mathrm{Bis}_3(a-x,\xi_1) + \frac{\pi}{4}\cos\phi_2 - \frac{\pi}{4}\cos\xi_2 + \mathrm{Cis}_3(b-y,\phi_2) - \mathrm{Cis}_3(b-y,\xi_2) + \frac{\pi}{4}\sin\phi_3 + \frac{\pi}{4}\sin\xi_3 - \mathrm{Bis}_3(x,\phi_3) - \mathrm{Bis}_3(x,\xi_3) - \frac{\pi}{4}\cos\phi_4 + \frac{\pi}{4}\cos\xi_4 - \mathrm{Cis}_3(y,\phi_4) + \mathrm{Cis}_3(y,\xi_4) \quad (A.10)$$

and

$$V(x,y) = -\frac{\pi}{4}\cos\phi_1 + \frac{\pi}{4}\cos\xi_1 - \mathrm{Cis}_3(a-x,\phi_1) + \mathrm{Cis}_3(a-x,\xi_1) - \frac{\pi}{4}\sin\phi_2 - \frac{\pi}{4}\sin\xi_2 + \mathrm{Bis}_3(b-y,\phi_2) + \mathrm{Bis}_3(b-y,\xi_2) + \frac{\pi}{4}\cos\phi_3 - \frac{\pi}{4}\cos\xi_3 + \mathrm{Cis}_3(x,\phi_3) - \mathrm{Cis}_3(x,\xi_3) + \frac{\pi}{4}\sin\phi_4 + \frac{\pi}{4}\sin\xi_4 - \mathrm{Bis}_3(y,\phi_4) - \mathrm{Bis}_3(y,\xi_4) \quad (A.11)$$

These functions can be calculated once and stored so that in an iterative solution algorithm repeated computations are not needed.

References

[1] S.K. Layolka, R.W. Tsai, A numerical method for solving integral equations of neutron transport-II, Nucl. Sci. Eng. 58 (1975) 317–328.

[2] A.L. Crosbie, R.G. Schrenker, Radiative transfer in a two-dimensional rectangular medium exposed to diffuse radiation, J. Quant. Spectrosc. Radiat. Transfer 31 (4) (1984) 339–372.

[3] Z. Altaç, The SK_N approximation for solving radiative transfer problems in absorbing, emitting, and isotropically scattering plane-parallel medium: Part 1, ASME J. Heat Transfer 124 (4) (2002) 674–684.

[4] Z. Altaç, The SK_N approximation for solving radiative transfer problems in absorbing, emitting, and linearly anisotropically scattering plane-parallel medium: Part 2, ASME J. Heat Transfer 124 (4) (2002) 685–695.

[5] Z. Altaç, Radiative transfer in absorbing, emitting and linearly anisotropic scattering inhomogeneous cylindrical medium, J. Quant. Spectrosc. Radiat. Transfer 77 (2) (2003) 177–192.

[6] S.T. Thynell, M.N. Özışık, Radiation transfer in an isotropically scattering homogeneous solid sphere, J. Quant. Spectrosc. Radiat. Transfer 33 (4) (1985) 319–330.

[7] S.T. Thynell, M.N. Özışık, Radiation transfer due to a point source in an isotropically scattering inhomogeneous solid sphere, J. Quant. Spectrosc. Radiat. Transfer 35 (5) (1986) 349–356.

[8] S. Wu, C. Wu, Partition-extrapolation integration applied to radiative transfer in cylindrical media, J. Quant. Spectrosc. Radiat. Transfer 48 (3) (1992) 279–286.

[9] J.M. Zhang, W.H. Sutton, Multidimensional radiative transfer in absorbing, emitting and linearly anisotropic scattering cylindrical medium with space-dependent properties, J. Quant. Spectrosc. Radiat. Transfer 52 (6) (1994) 791–808.

[10] M. Abramowitz, I.A. Stegun, Handbook of Mathematical Functions, Dover Publications Inc., New York, 1964, p. 483.

[11] E.E. Lewis, W.F. Miller, Computational Methods of Neutron Transport, John Wiley & Sons, Inc., 1984, pp. 166–175.

[12] DOQDP-Discrete Ordinates Quadrature Generator, RSIC Code Package PSR-110, ORNL, 1977.

[13] Z. Altaç, Integrals involving Bickley and Bessel functions in radiative transfer and generalized exponential integral function, ASME J. Heat Transfer 118 (3) (1996) 789–791.